Electronic supplementary information

Rational design of potential spin qubits manipulated by valence tautomerism mechanism: quantum-chemical modeling of the trinuclear transition metal complexes with bischelate linkers

Alyona A. Starikova and Vladimir I. Minkin

New Journal of Chemistry

The details of the DFT UB3LYP*/6-311++G(d,p) calculations of the complexes 3–5 (X = O, NR'; R = H, CH_3, CF_3; R' = H, CH_3, Ph)

As follows form the computational results, the compounds with cobalt diketonates **3** (X=O; R=H, CH_3, CF_3) are stable ($E_{стаб}$ = 6.1-21.9 kcal mol^{-1}) with respect to dissociation into the isolated components (Table S1). The low-spin $_{LS}Co^{III}$-SQ structures **S1** and **S3**, in which spin density is mostly localized at redox-active ligand in semiquinonate (SQ) form (Fig. S1) correspond to the ground state of mixed-ligand Co^{II} bis-malonate and bis-acetylacetonate complexes **3** (X=O; R=H, CH_3). The high-spin isomers **S2** and **S4** comprising $_{HS}Co^{II}$ are destabilized as compared to the low-spin electomers by more than 10 kcal mol^{-1}, which does not allow to expect the occurrence of valence-tautomeric (VT) rearrangements. Insertion into the diketonate moiety of electron-withdrawing trifluoromethyl groups results in increasing the stability of the adducts **3** (X=O; R= CH_3, CF_3) and narrowing the energy gap between the low-spin and the high-spin isomers to the value 6.4 kcal mol^{-1}, which indicates the possibility of intramolecular redox-process. Close values of total energies of the isomers **S7** and **S8** of the complex **3** (R=CF_3) witness on probable co-existence of both forms in solution.

Table S1. Spin (S), total energies (E_{total}), stabilization energies (E_{stab}), relative energies (ΔE) and spin density at cobalt ion (q_s^{Co}) in the electromeric forms of the adducts of Co^{II} diketonates **3** (X=O; R=H, CH_3, CF_3) calculated by DFT UB3LYP*/6-311++G(d,p) method.

Structure	S	E_{total}, a. u.	E_{stab}, kcal mol^{-1}	ΔE, kcal mol^{-1}	q_s^{Co}, a. u.
S1 $_{LS}Co^{III}$-SQ	1/2	-2881.82403	18.9	0.0	0.01
S2 $_{HS}Co^{II}$-Q	3/2	-2881.80688	8.2	10.8	2.78
S3 $_{LS}Co^{III}$-SQ	1/2	-3039.04386	18.5	0.0	0.04
S4 $_{HS}Co^{II}$-Q	3/2	-3039.02405	6.1	12.4	2.81
S5 $_{LS}Co^{III}$-SQ	1/2	-3634.42334	19.3	0.0	0.04
S6 $_{HS}Co^{II}$-Q	3/2	-3634.41314	12.9	6.4	2.75
S7 $_{LS}Co^{III}$-SQ	1/2	-4229.79372	21.5	0.0	0.05
S8 $_{HS}Co^{II}$-Q	3/2	-4229.79433	21.9	-0.4	2.73

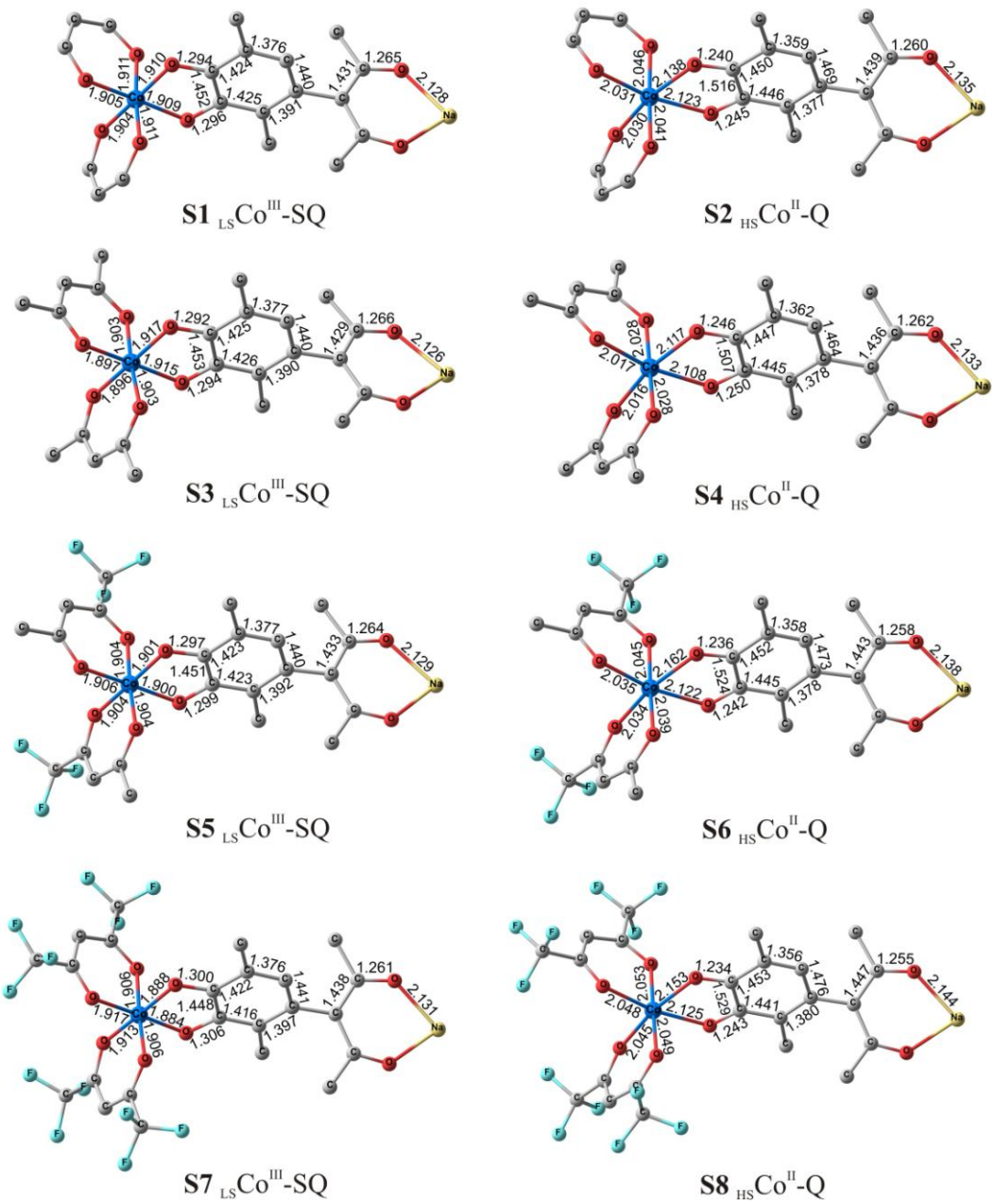

Figure S1. Optimized geometries of the electromeric forms of adducts **3** (X=O; R=H, CH_3, CF_3) calculated by the DFT B3LYP*/6-311++G(d,p) method. Hereafter bond lengths are given in Å, hydrogen atoms are omitted for clarity.

The most stable forms (**S9**, **S12** and **S15**) of the adducts **4** (X=NR'; R'=H, CH_3, Ph) of cobalt(II) bis-salicylaldiminates have the low-spin $_{LS}Co^{III}$-SQ electronic state (Fig. S2, Table S2). The high-spin isomers **S10**, **S13** and **S16** comprising $_{HS}Co^{II}$ are disfavored as compared to the low-spin ones by more than 12 kcal mol^{-1} and characterized by low stability against to dissociation (E_{stab} < 1 kcal mol^{-1}). Structures (**S11**, **S14** and **S17**) comprising semiquinolate and three-charged cobalt ion in the intermediate-spin state have also been found on the quartet potential energy surface. The predicted energy characteristics of the isomers point to impossibility of VT in adducts **4** (X=NR'; R'=H, CH_3, Ph).

Table S2. Spin (S), total energies (E_{total}), stabilization energies (E_{stab}), relative energies (ΔE) and spin density at cobalt ion (q_s^{Co}) in the electromeric forms of the adducts of Co^{II} bis-aminovinylketonates **4** (X=NR'; R'=H, CH_3, Ph) calculated by DFT UB3LYP*/6-311++G(d,p) method.

Structure	S	E_{total}, a. u.	E_{stab}, kcal mol^{-1}	ΔE, kcal mol^{-1}	q_s^{Co}, a. u.
S9 $_{LS}Co^{III}$-SQ	1/2	-2842.08383	16.7	0.0	0.03
S10 $_{HS}Co^{II}$-Q	3/2	-2842.05317	-2.6	19.2	2.85
S11 $_{IS}Co^{III}$-SQ	3/2	-2842.06391	4.2	12.5	1.71
S12 $_{LS}Co^{III}$-SQ	1/2	-2920.65457	17.9	0.0	0.06
S13 $_{HS}Co^{II}$-Q	3/2	-2920.62700	0.6	17.3	2.84
S14 $_{IS}Co^{III}$-SQ	3/2	-2920.63514	5.7	12.2	1.71
S15 $_{LS}Co^{III}$-SQ	1/2	-3303.96736	14.5	0.0	0.04
S16 $_{HS}Co^{II}$-Q	3/2	-3303.94448	0.2	14.4	2.74
S17 $_{IS}Co^{III}$-SQ	3/2	-3303.94579	1.0	13.5	1.72

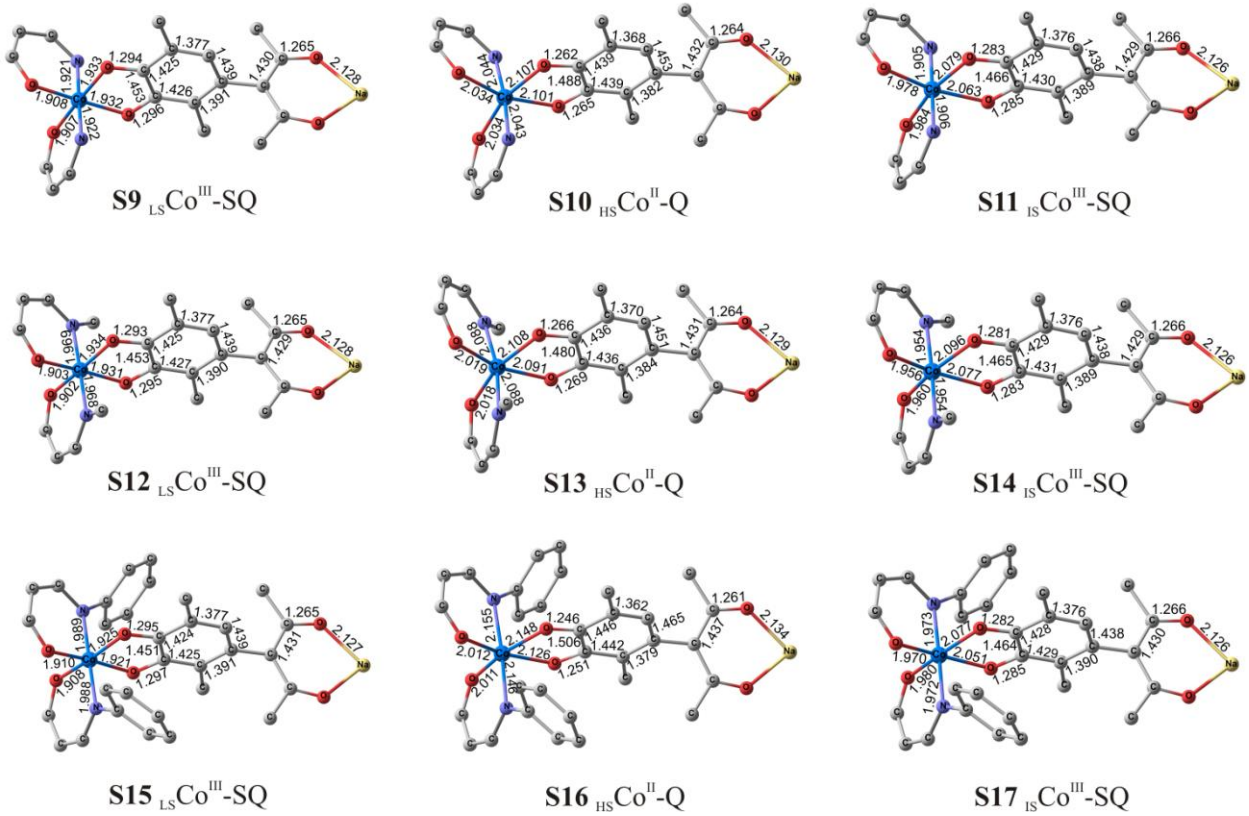

Figure S2. Optimized geometries of the electromeric forms of adducts **4** (X=NR'; R'=H, CH_3, CF_3) calculated by the DFT B3LYP*/6-311++G(d,p) method.

The results of calculations of mixed-ligand complexes **5** (X=NR'; R'=H, CH_3, Ph) are similar to those obtained for the adducts with Co^{II} bis-aminovinylketonates (Fig. S3): the significant stabilization of the low-spin $_{LS}Co^{III}$-SQ isomers (**S18**, **S21** and **S24**) and energy preference of the $_{IS}Co^{III}$-SQ forms comprising Co^{III} in the intermediate-spin state (**S20**, **S23** and **S26**) as compared to the $_{HS}Co^{II}$-Q structure with the high-spin Co^{II} (**S19**, **S22** and **S25**) do not allow to expect the occurrence of VT transitions in adducts of Co^{II} bis-salicylaldiminates.

Table S3. Spin (S), total energies (E_{total}), stabilization energies (E_{stab}), relative energies (ΔE) and spin density at cobalt ion (q_s^{Co}) in the electromeric forms of the adducts of Co^{II} bis-salicylaldiminates **5** (X=NR'; R'=H, CH_3, Ph) calculated by DFT UB3LYP*/6-311++G(d,p) method.

Structure	S	E_{total}, a. u.	E_{stab}, kcal mol^{-1}	ΔE, kcal mol^{-1}	q_s^{Co}, a. u.
S18 $_{LS}Co^{III}$-SQ	1/2	-3149.23973	14.3	0.0	0.04
S19 $_{HS}Co^{II}$-Q	3/2	-3149.21078	-3.8	18.2	2.85
S20 $_{IS}Co^{III}$-SQ	3/2	-3149.22150	2.9	11.4	1.67
S21 $_{LS}Co^{III}$-SQ	1/2	-3227.81305	19.2	0.0	0.09
S22 $_{HS}Co^{II}$-Q	3/2	-3227.78762	3.3	16.0	2.81
S23 $_{IS}Co^{III}$-SQ	3/2	-3227.79643	8.8	10.4	1.66
S24 $_{LS}Co^{III}$-SQ	1/2	-3611.12338	30.7	0.0	0.09
S25 $_{HS}Co^{II}$-Q	3/2	-3611.10278	17.8	12.9	2.66
S26 $_{IS}Co^{III}$-SQ	3/2	-3611.10416	18.7	12.1	1.72

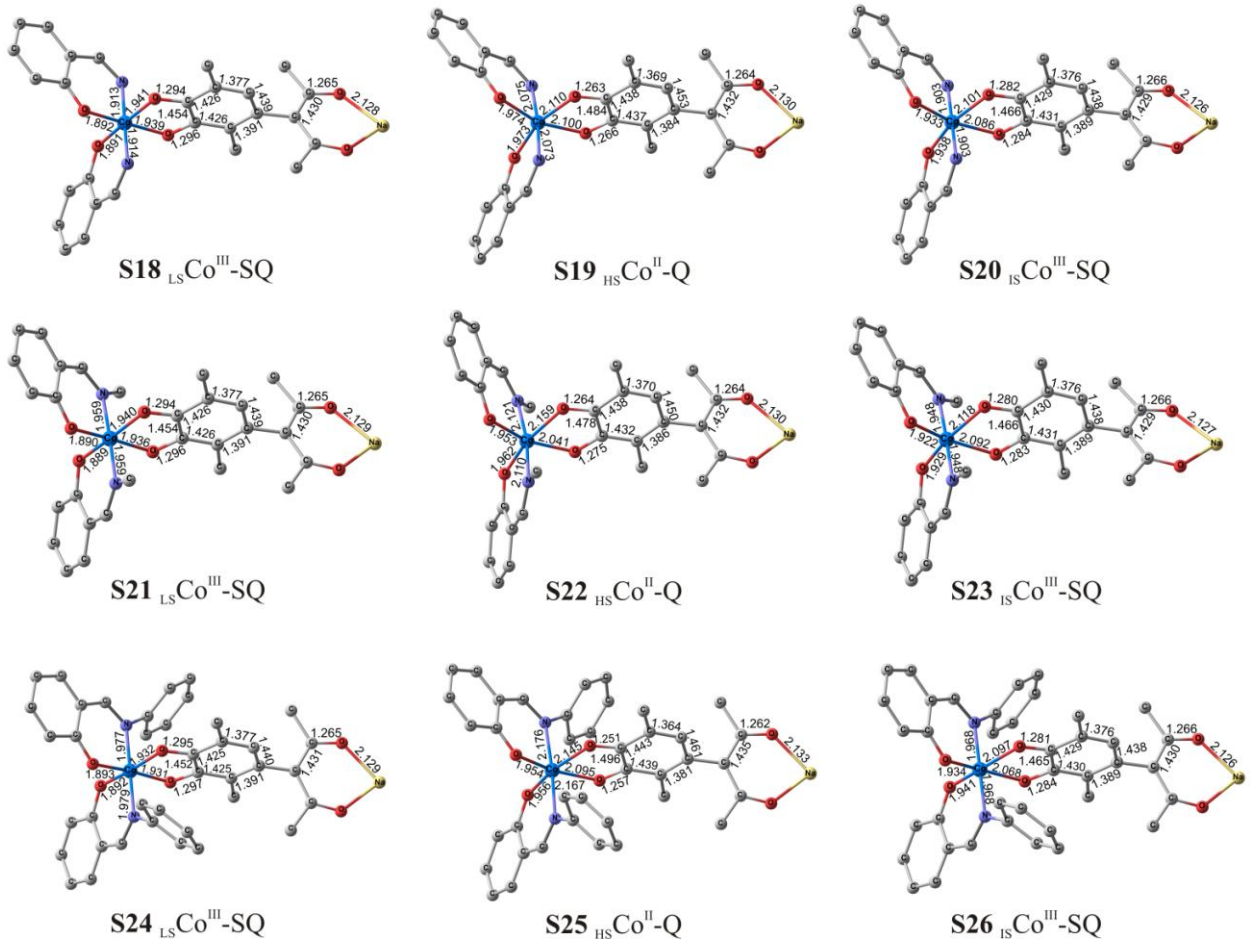

Figure S3. Optimized geometries of the electromeric forms of adducts **5** (X=NR'; R'=H, CH_3, CF_3) calculated by the DFT B3LYP*/6-311++G(d,p) method.

Table S4. Spin (S), total energies without (E_{total}) and with (E_{total}^{ZPE}) taking account of energies of zero harmonic vibrations, expectation values of spin-squared (S^2) operator of the adducts **2** (M=Cu; X=O; R=CH_3, CF_3) calculated by DFT B3LYP*/6-311++G(d,p) method.

Structure		S	E_{total}	E_{total}^{ZPE}	S^2
			a. u.		
7 $_{LS}Co^{III}$-SQ-Cu^{II}-SQ-$_{LS}Co^{III}$	**ααα**[a]	3/2	-7393.86416	-7392.94957	3.76
	ααβ	1/2	-7393.86427		1.76
	αβα	1/2	-7393.86437		1.76
8 $_{LS}Co^{III}$-SQ-Cu^{II}-Q-$_{HS}Co^{II}$	**ααα**	5/2	-7393.84183	-7392.93142	9.17
	βαα	3/2	-7393.84194		5.16
	αβα	3/2	-7393.84187		5.16
	ββα	1/2	-7393.84176		3.17
9 $_{HS}Co^{II}$-Q-Cu^{II}-Q-$_{HS}Co^{II}$	**ααα**	7/2	-7393.81905	-7392.91240	16.61
	αβα	5/2	-7393.81893		10.61
	ααβ	1/2	-7393.81899		4.61
10 $_{LS}Co^{III}$-SQ-Cu^{II}-SQ-$_{LS}Co^{III}$	**ααα**	3/2	-9775.35776	-9774.62633	3.76
	ααβ	1/2	-9775.35790		1.76
	αβα	1/2	-9775.35805		1.75
11 $_{LS}Co^{III}$-SQ-Cu^{II}-Q-$_{HS}Co^{II}$	**ααα**	5/2	-9775.35290	-9774.62483	8.82
	βαα	3/2	-9775.35304		4.82
	αβα	3/2	-9775.35301		4.82
	ββα	1/2	-9775.35287		2.82
12 $_{HS}Co^{II}$-Q-Cu^{II}-Q-$_{HS}Co^{II}$	**ααα**	7/2	-9775.34631	-9774.62224	15.90
	αβα	5/2	-9775.34627		9.90
	ααβ	1/2	-9775.34629		3.91
13 MECP			-9775.33863		
14 MECP			-9775.33686		

[a] **α** – spin up, **β** – spin down

Table S5. Spin (S), total energies without (E_{total}) and with (E_{total}^{ZPE}) taking account of energies of zero harmonic vibrations, expectation values of spin-squared (S^2) operator of the adduct **2** (M=$_{HS}$Co; X=O; R=CF_3) calculated by DFT B3LYP*/6-311++G(d,p) method.

Structure		S	E_{total}	E_{total}^{ZPE}	S^2
			a. u.		
15 $_{LS}$Co^{III}-SQ-$_{HS}$Co^{II} $_{(linker)}$-SQ-$_{LS}$Co^{III}	**ααα**[a]	5/2	-9517.66888	-9516.93747	8.77
	ααβ	3/2	-9517.66903		4.77
	βαβ	1/2	-9517.66917		2.77
16 $_{LS}$Co^{III}-SQ-$_{HS}$Co^{II} $_{(linker)}$-Q-$_{HS}$Co^{II}	**ααα**	7/2	-9517.66379	-9516.93592	15.84
	βαα	5/2	-9517.66391		9.83
	αβα	1/2	-9517.66386		3.83
	ααβ	1/2	-9517.66374		3.83
17 $_{HS}$Co^{II}-Q-$_{HS}$Co^{II} $_{(linker)}$-Q-$_{HS}$Co^{II}	**ααα**	9/2	-9517.65734	-9516.93309	24.92
	αβα	3/2	-9517.65727		6.91
	ααβ	3/2	-9517.65730		6.91

[a] **α** – spin up, **β** – spin down

Table S6. Spin (S), total energies (E_{total}), stabilization energies (E_{stab}), relative energies (ΔE), expectation values of spin-squared (S^2) operator and exchange spin coupling constants (J^a) of the electromeric forms of the adducts **2** (M=$_{LS}$Ni, Zn; X=O; R=CF_3) calculated by the DFT B3LYP*/6-311++G(d,p) method.

Structure	S	E_{total}, a. u.	E_{stab}	ΔE	S^2	J, cm^{-1}
			kcal mol^{-1}			
18 $_{LS}$Co^{III}-SQ-$_{LS}$Ni^{II}-SQ-$_{LS}$Co^{III}	2/2	-9643.19992	43.5	0.0	2.013	
BS		-9643.19991			1.014	0.1
19 $_{LS}$Co^{III}-SQ-$_{LS}$Ni^{II}-Q-$_{HS}$Co^{II}	4/2	-9643.19499	40.4	3.1	6.074	
BS		-9643.19499			3.074	0.0
20 $_{HS}$Co^{II}-Q-$_{LS}$Ni^{II}-Q-$_{HS}$Co^{II}	6/2	-9643.18821	36.1	7.3	12.156	
21 $_{LS}$Co^{III}-SQ-Zn^{II}-SQ-$_{LS}$Co^{III}	2/2	-9914.21538	43.3	0.0	2.013	
BS		-9914.21538			1.013	0.0
22 $_{LS}$Co^{III}-SQ-Zn^{II}-Q-$_{HS}$Co^{II}	4/2	-9914.21024	40.1	3.2	6.074	
BS		-9914.21024			3.074	0.0
23 $_{HS}$Co^{II}-Q-Zn^{II}-Q-$_{HS}$Co^{II}	6/2	-9914.20390	36.1	7.2	12.153	

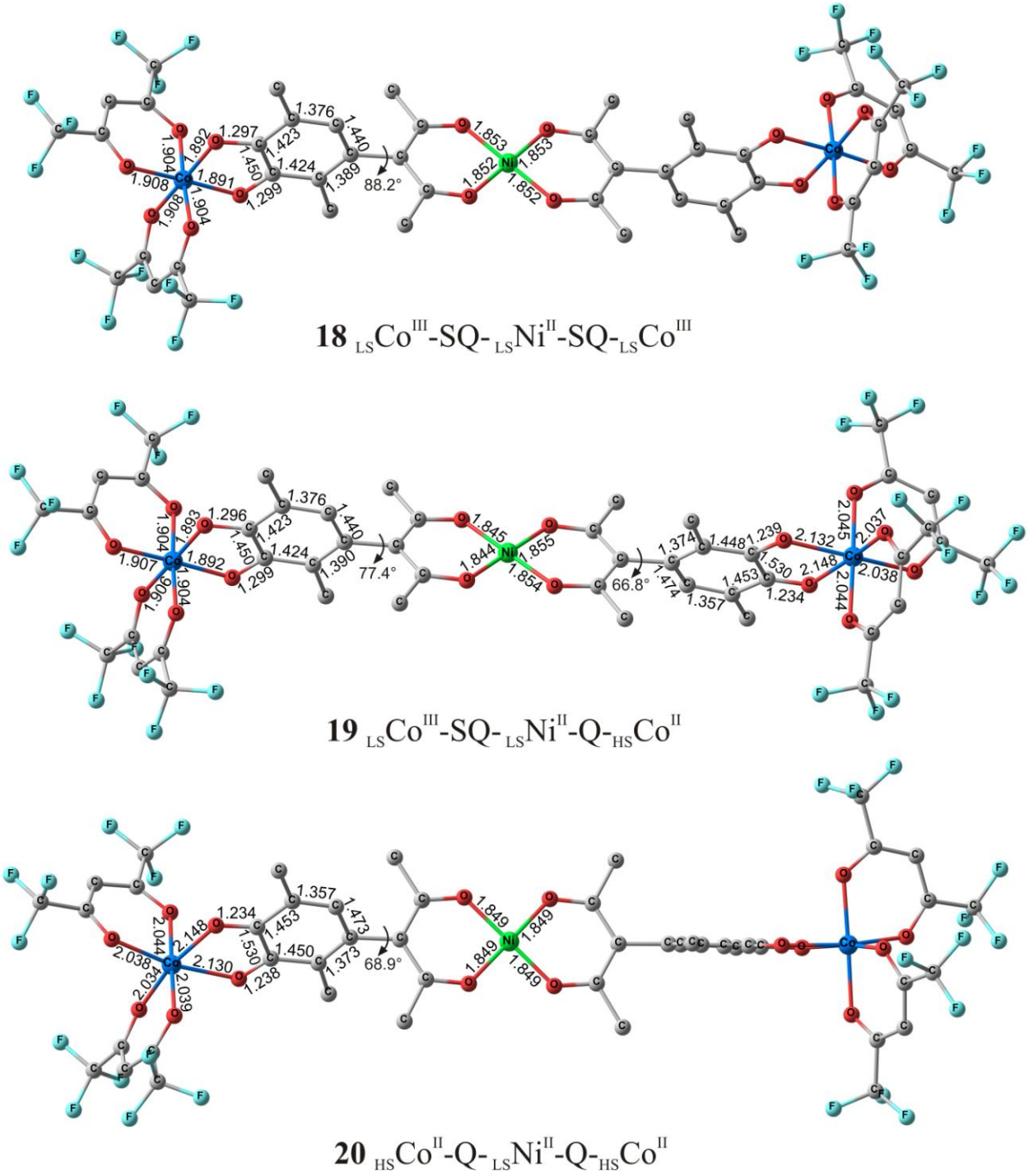

Figure S4. Optimized geometries of the electromeric forms of adducts **2** (M=$_{LS}$Ni; X=O; R=CF_3) calculated by the DFT B3LYP*/6-311++G(d,p) method.

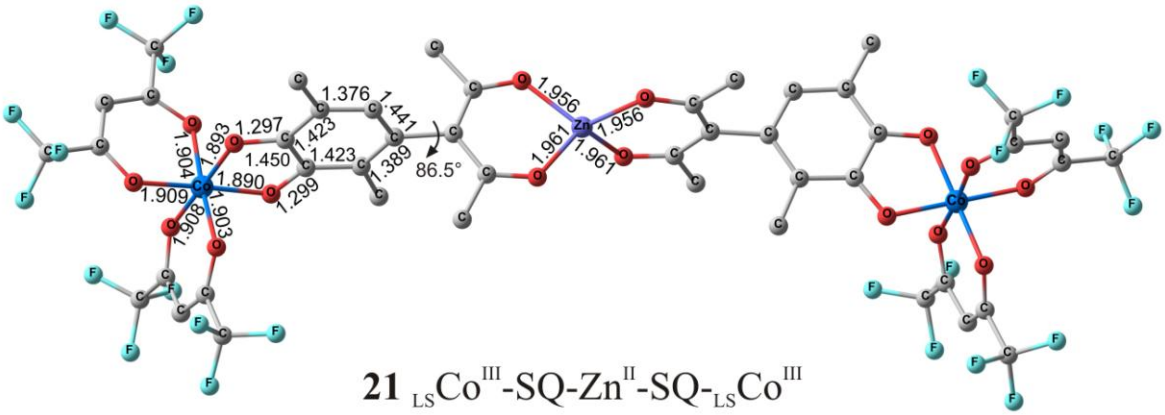

21 $_{LS}Co^{III}$-SQ-Zn^{II}-SQ-$_{LS}Co^{III}$

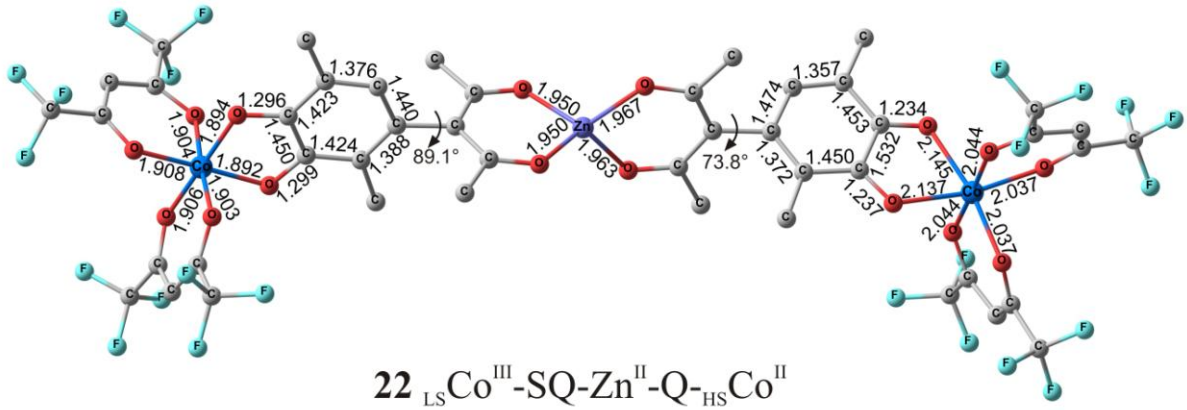

22 $_{LS}Co^{III}$-SQ-Zn^{II}-Q-$_{HS}Co^{II}$

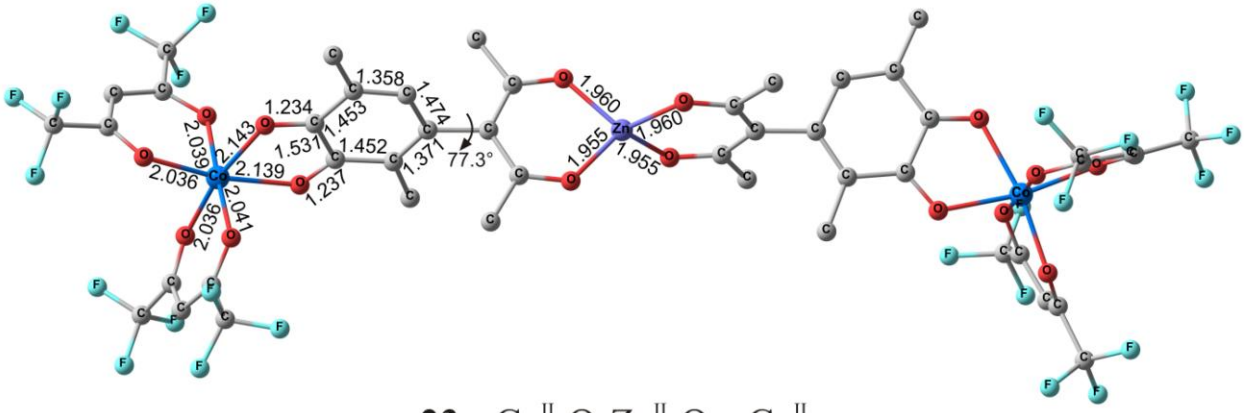

23 $_{HS}Co^{II}$-Q-Zn^{II}-Q-$_{HS}Co^{II}$

Figure S5. Optimized geometries of the electromeric forms of adducts **2** (M= Zn; X=O; R=CF_3) calculated by the DFT B3LYP*/6-311++G(d,p) method.

Table S7. Spin (*S*) and total energies (E_{total}) of the cobalt bischelates and redox-active ligands calculated by the DFT B3LYP*/6-311++G(d,p) method.

Structure	S	E_{total}, a. u.
$Cobalt^{II}$ bis-malonate	3/2	-1915.67070
$Cobalt^{II}$ bis-acetylacetonate	3/2	-2072.89123
$Cobalt^{II}$ bis-trifluoroacetylacetonate	3/2	-2668.26938
$Cobalt^{II}$ bis-hexafluoroacetylacetonate	3/2	-3263.63635
$Cobalt^{II}$ bis-aminovinylketonate	1/2	-1875.93416
$Cobalt^{II}$ N-methyl-bis-aminovinylketonate	3/2	-1954.50293
$Cobalt^{II}$ N-phenyl-bis-aminovinylketonate	3/2	-2337.82108
$Cobalt^{II}$ bis-salicylaldiminate	1/2	-2183.09376
$Cobalt^{II}$ N-methyl-bis-salicylaldiminate	3/2	-2261.65926
$Cobalt^{II}$ N-phenyl-bis-salicylaldiminate	3/2	-2644.95127
3-(4’,5’-dihydroxy-3’,6’-dimethyl) phenylacetylacetonate of Na^{I}	0	-966.12314
Tetradentate redox-active ligand with ${}_{HS}Co^{II}$ bischelate linker	3/2	-2990.32723
Tetradentate redox-active ligand with ${}_{LS}Ni^{II}$ bischelate linker	0	-3115.85790
Tetradentate redox-active ligand with Cu^{II} bischelate linker	1/2	-3248.01596
Tetradentate redox-active ligand with Zn^{II} bischelate linker	0	-3386.87368